

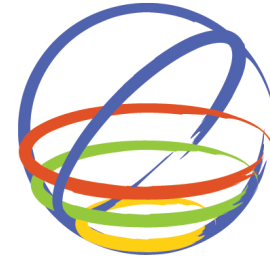
Probabilistic Tsunami Hazard Analysis

H.K. Thio & P.G. Somerville

URS Corp, Los Angeles, CA, USA

J. Polet

California State Polytechnic University, CA, USA



15 WCEE
LISBOA 2012

SUMMARY:

The large tsunami disasters of the last decade have highlighted the need for performance-based solutions to the problem of tsunami loading and thus the establishment of a probabilistic framework for tsunami hazard analysis. We have developed a method for Probabilistic Tsunami Hazard Analysis (PTHA) that closely follows, where possible, the approach in Probabilistic Seismic Hazard Analysis (PSHA) using a two-step approach.

First we compute fully probabilistic offshore waveheights. We use a library of pre-computed tsunami Green's functions from all potential sources, which allows us to integrate over a wide range of locations and magnitudes, similar to PSHA, and also incorporate epistemic uncertainties through the use of logic trees and aleatory uncertainties using distribution functions.

In the second step, we compute inundation scenarios using a small subset of events, based on source disaggregation, of events that are representative of the hazard expressed by the probabilistic waveheights derived in step 1. This process has enabled us to develop probabilistic tsunami inundation maps for California.

Keywords: Tsunamis, Hazard, Inundation, Probabilistic

1. INTRODUCTION

Since the tsunami disaster caused by the 2004 Sumatra-Andaman earthquake (Ammon et al. 2005), which has focused our attention on the hazard posed by tsunamis generated by large subduction zone earthquakes, the need has become clear for a systematic evaluation of tsunami hazard. Even before this destructive event, a significant amount of work was carried out in this field, primarily through deterministic modeling of tsunami scenarios (e.g., Borrero et al. 2005). Such studies usually address worst-case scenarios or some type of maximum credible event. For a wide variety of applications, such as performance based engineering, land-use planning, etc. it is however desirable to be able to express the hazard in probabilistic terms, and in this paper we present a method for probabilistic tsunami hazard analysis (PTHA) that not only yields probabilistic offshore waveheights but also inundation.

Also, notwithstanding the great usefulness of individual scenario maps, in order to assess the hazard for a certain region, it may be more appropriate to start with a map of the tsunami hazard, analogous to the seismic hazard maps that are published by government agencies such as the United States Geological Survey and statewide agencies in the U.S., or the Global Seismic Hazard Assessment Program. Even though events like the Sumatra-Andaman earthquake and tsunami are rare, the very large loss of life (> 200,000 dead or missing) and tremendous material destruction over large geographical areas warrant a significant effort towards the mitigation of the tsunami hazard worldwide. In recent years, the tsunami risk posed to United States coastal communities from a variety of sources has also become apparent with the need for a comprehensive and consistent methodology to evaluate this aspect of earthquake risk that so far has been neglected. On the other hand, where there is concern about tsunami damage, the lack of a

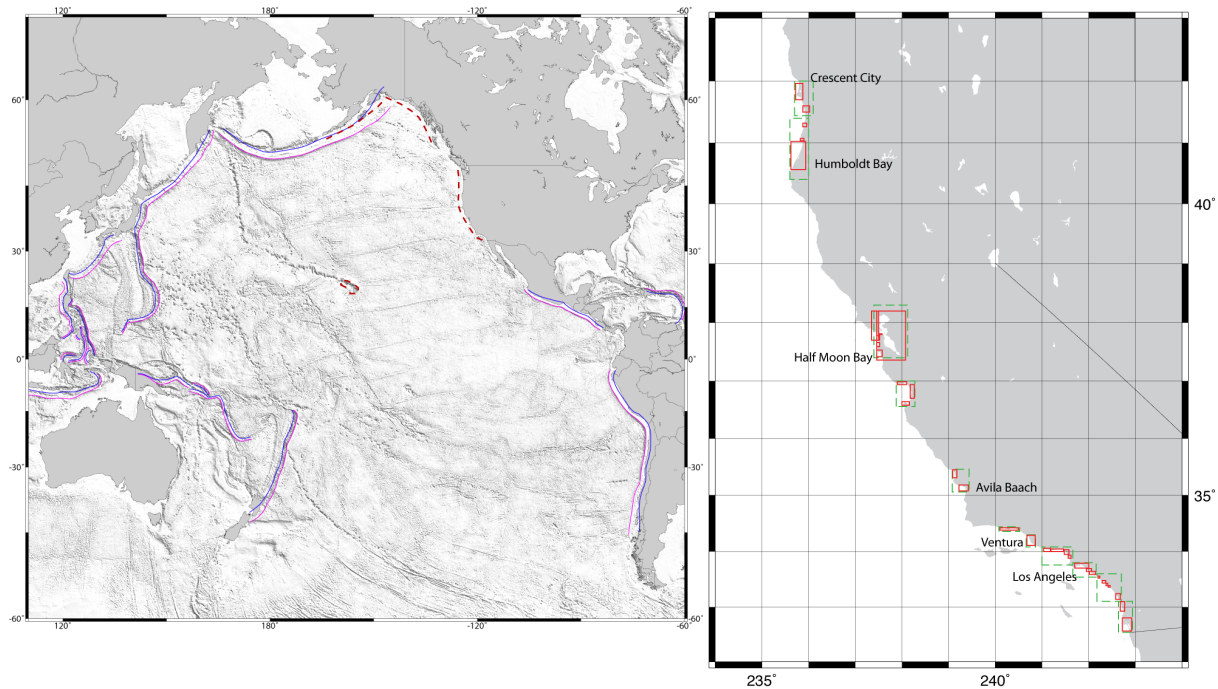


Figure 1.1. Source distribution along the Pacific Rim used in this study (left), and the location of the detailed tsunami inundation analysis (right).

consistent framework to evaluate this hazard has given rise to unnecessarily conservative estimates, which can result in an economic barrier to development of coastal communities and facilities.

2. TSUNAMI MODELING

Although we would like to follow seismic practice closely, there is a fundamental difference between tsunami hazard analysis and seismic hazard analysis in terms of the forward modelling problem. Seismic ground motion can be expressed by relatively simple functions of distance between site and source, magnitude and a limited number of second-order parameters (i.e. ground motion prediction equations). For tsunami propagation, such an approach is not practical, given the large lateral variations in the propagating medium, the oceans. On the other hand, the main parameter governing the tsunami propagation, water depth, is generally very well known, making it feasible to model tsunami waves numerically to a much higher accuracy than is currently possible for seismic waves. In the following section, we shall briefly explain the numerical methods that we used in our approach.

We take a Eulerian approach to describe the particle motion of the fluid. Only the velocity changes of the fluid are described at some point and at some instant of time rather than describing its absolute displacement. We consider a wave that is a propagating disturbance from an equilibrium state. Gravity waves occur when the only restoring force is gravity. When the horizontal scale of motion is much larger than the water depth, then the vertical acceleration of water is much smaller than the gravity acceleration and thus negligible. This means that the whole water mass from the bottom to the surface is assumed to move uniformly in a horizontal direction. This kind of gravity wave is also known as a “long-wave.” Long wave approximations are appropriate when the water depth of lakes and oceans (< 5 km) is much smaller than the length of the disturbance (fault lengths ~ 10 -1000 km). This approximation gives an accurate description of tsunami wave propagation in the open ocean. In order to also model the propagation of

tsunami waves in coastal areas, we use an approximation to the wave equation where the low-amplitude linear long-wave requirements are relaxed.

Numerical Computation

The equations of motion and equation of continuity are implemented in a spherical coordinate system. They are solved by a finite-difference method using the staggered leapfrog method (e.g., Satake, 1995). For the advection terms, an upwind difference scheme is used. The land-sea is a moving boundary condition so that inundation and run-up are included. The time step of computation is determined by trial and error. This code has been used by various researchers (e.g. Ichinose et al., 2007; Baba et al, 2004; Fuji et al., 2006; Burbidge et al, 2008; Baba et al., 2008) and has been validated against several benchmarks and other codes.

Variable grid finite difference

The variable grid setup consists of a master grid with a coarse grid spacing and a number of nested finer grids with decreasing grid sizes around areas of interest. Our code allows for more than one area with decreased grid size. In this model, the deep ocean part is sampled at 120 arc seconds. Because of the very long wavelength of tsunami waves in the deep ocean, such a sampling is sufficient for accurate results and reduces the computation time and memory requirements considerably. Closer to shore, we used several nested grids stepping down to .96 arc sec (approx 30 m). The timestep for these runs is 0.5 sec. Currently, our code uses a fixed timestep, which generally is controlled by the finest gridsize.

3. PROBABILISTIC HAZARD ANALYSIS

Offshore hazard

The methodology behind probabilistic seismic hazard analysis (PSHA) is well known (e.g., McGuire 2004) and here we will only briefly describe the adaptations that are made for tsunamis (PTHA). Whereas in PSHA we are usually interested in the exceedance of some ground motion measure such as peak ground acceleration (PGA) or spectral acceleration (SA), in PTHA a parameter of interest (not necessarily the only one) is the maximum tsunami height at sites along the coast. The statistical earthquake model behind the two methods is the same, the only difference being that in PTHA we are not concerned with earthquakes that are completely inland and in general the minimum magnitude of interest tends to be much higher (e.g. $M=5$ for seismic hazard vs $M=7$ for tsunami hazard). The difference between the two methods lies in the part that in PSHA is referred to as attenuation relations. These relate a certain seismic moment release on a fault (or an area) to the ground motion parameters as a function of distance. Because of the strong laterally varying nature of tsunami propagation, we have adopted a waveform excitation and propagation approach instead of trying to develop analogous tsunami attenuation relations. In fact, current developments in traditional PSHA include the replacement of the attenuation relations with ensembles of numerically generated ground motions, which is entirely analogous to the approach used here. The method has been used by Burbidge et al. (2008) to map probabilistic tsunami hazard around Australia, and Thio et al. (2010) to map probabilistic tsunami inundation in California.

The excitation and propagation of tsunamis in deeper water can be modeled using the shallow water wave approximation, which for amplitudes that are significantly smaller than the water depth are linear (Satake 1995). We can solve the equation of motion numerically using a finite-difference method, which has been validated to produce accurate tsunami heights for propagation through the oceans, although for very shallow water the amplitudes may become too large, and more sophisticated nonlinear methods are required to model the details of the run-up accurately. Nevertheless, the linear approach provides a very

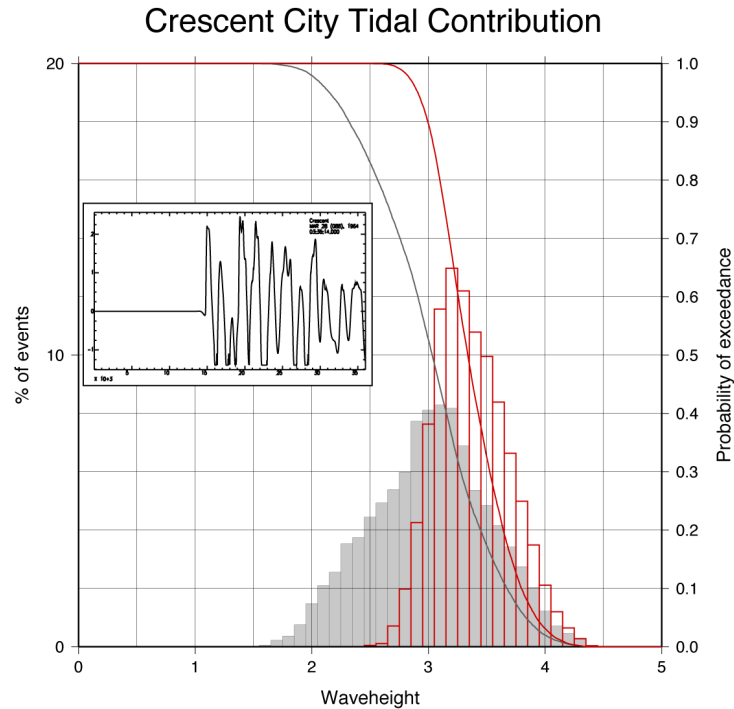


Figure 3.1. Example of the effect of tides on the probabilistic exceedance waveheight. The grey histograms show the probability density function of the tidal record superposed on a simulated maximum waveheight of 3 m. The grey curve shows the corresponding cumulative density function, or probability of exceedance given a modeled maximum waveheight and the observed tide record. The tsunami simulation (inset, showing 10 hr record) however shows multiple peaks close to the maximum waveheights and the correct way to take the multiple peaks into account is to convolve the simulated timeseries with the tidal record which in this case yield significantly larger exceedance waveheights for the same probability.

good first approximation of tsunami propagation for the offshore waveheight.

Aleatory uncertainties

Aleatory uncertainties reflect the inability to predict the outcome of a process due to its random nature. Whether or not an uncertainty in the outcome of a process is a true aleatory uncertainty, i.e., caused by the random behavior of nature rather than a limited understanding of the process itself, is not always clear. In practice, this distinction is not important. Aleatory uncertainties are typically accounted for by the use of distribution functions rather than single mean or median values to express the outcome of a process. The probability of an outcome being in a certain range is then given by the area under the probability density (or distribution) function. In our analysis we have identified three main contributions to the aleatory uncertainty: modeling uncertainty (σ_A), uncertainty to random slip distribution (σ_S) and uncertainty due to the tidal variations at any location (σ_T).

2500 yr return period

Santa_Monica-475yr

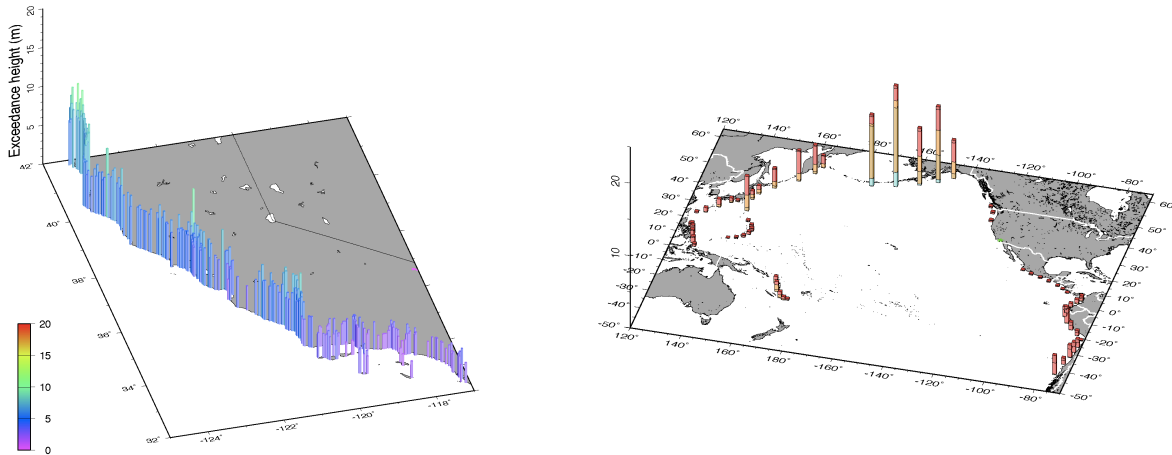


Figure 3.2 Offshore exceedance waveheights for California at a return period of 2500 yrs (left) from a fully probabilistic integration over all subduction sources in the Pacific. On the right we show the source disaggregation results for Santa Monica for a return period of 475 yrs. The hazard is dominated by source in Alaska, but there are also smaller contributions from source around Japan and Chile.

Under modeling uncertainty we include the mismatch, given known source parameters, between observed and computed tsunami waveforms. Several different sources contribute to this modeling uncertainty, the two most important being errors from the numerical implementation (i.e., our finite difference scheme) and errors from shortcomings in the bathymetric model (either errors in the model, or insufficient resolution). We have estimated this uncertainty by modeling several large and well-constrained tsunamis along the California coast, including the 1960 Chile, 1964 Alaska, and 2006 Kurile events, and by comparing the observed and computed maximum waveheights or run-ups. The standard deviations (σ_A) for coarse (1km) and fine (90m) grids are 0.595 and 0.345 (natural log), respectively. We truncated the standard deviation for the aleatory uncertainty at an epsilon of 3.

We take into account the source variability, such as uncertainties in scaling relations and maximum slip by directly sampling these parameter distributions using sources that have been perturbed accordingly. The variability in the scaling relations are usually given with the scaling relations themselves (e.g. Papazachos et al., 2004).

Variations in tide level can have a significant impact on the effective waveheight, and have to be taken into account. In Figure 3.1 we show the effect of tidal variations on the maximum waveheights. In simple cases, we can deal with this problem by replacing the computed waveheight at any point by the probability density function of the tides. While this works for a tsunami wave with one isolated and unique peak, it underestimates the hazard when the tsunami has several peaks with amplitudes comparable to the maximum waveheight. In this case, there is a larger chance that a particular waveheight is exceeded since there are now several peaks that can coincide with a tidal high.

Epistemic uncertainties

Uncertainties in the model parameters are generally incorporated using a logic-tree approach, where different alternatives are represented as weighted branches. These include variations in slip-rate, magnitude range and distribution, fault geometry, as well as rake.

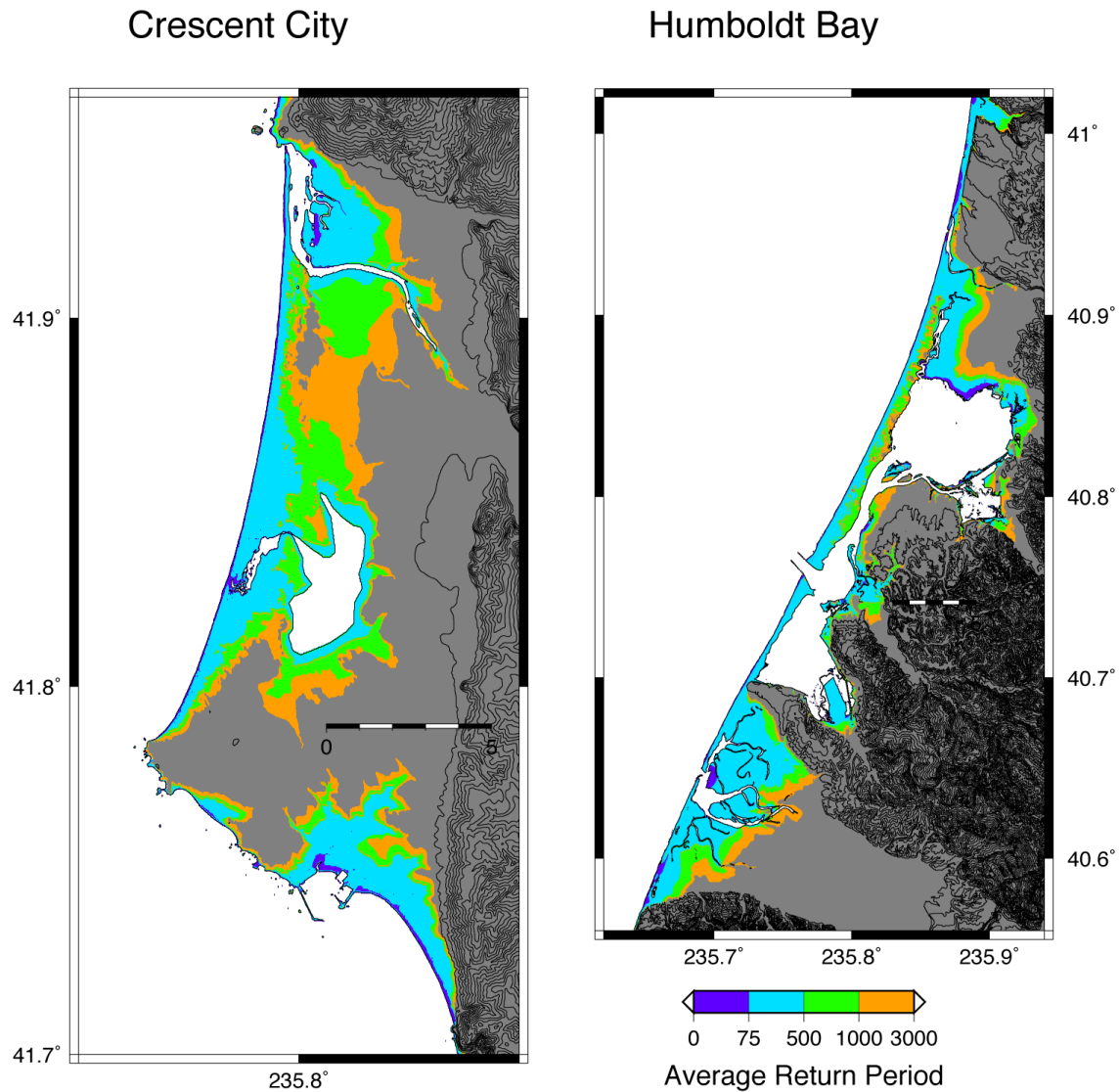


Figure 4.1 Probabilistic tsunami inundation map for two areas along the Cascadia coast of California, Crescent City (left) and Humboldt Bay (right). The colors indicate the average return time for inundation.

In the Green's function approach, it is convenient to divide these uncertainties into two groups: parameter variations that act on the Green's function level (e.g., fault geometry) and parameters that do not influence the Green's functions, such as the recurrence parameters and magnitude scaling relations. In the latter case, the logic tree branches are easily added without major computational requirements, but for the former, the question is whether any extra branch in the logic tree, such as a variation in slip, would require an entire set of Green's functions. From some simple numerical experiments, we conclude that in many cases, especially at large distances, these variations can accurately be taken into account by perturbing the Green's functions using a constant scaling factor rather than re-computing them. For example, a change in rake, readily translates into a change of the vertical seafloor displacement, which in turn directly translate to differences in waveheight.

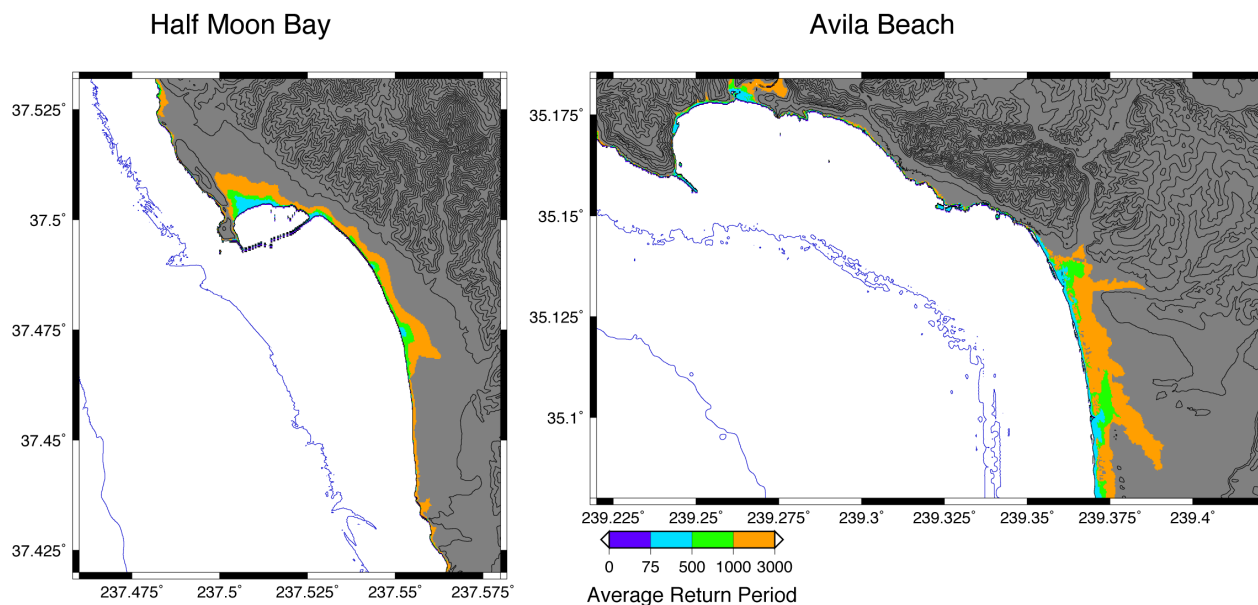


Figure 4.2. Probabilistic inundation map two sites in Central California, Half Moon Bay (left) and Avila Beach (right).

At shorter distances, i.e., local faults, this approach is less accurate, and in these situations (particularly for dip-slip events) we will have to resort to complete re-computation of the Green's functions. However, since these sources are relatively scarce, and require less computing time due to the short distances, this is far less of a burden than having to re-compute tele-tsunami Green's functions.

Probabilistic offshore hazard

In Figure 3.2 we present an example of the offshore waveheight off California for a return period of 2500 yr. These waveheights have been calculated for a depth of 30 m and give a good overview of the relative hazard along the coast. It is clear that the hazard is highest in Cascadia and lowest in Southern California. The disaggregation meanwhile gives us a good idea what the main contributions are to the hazard.

4. PROBABILISTIC INUNDATION HAZARD

In order to extend the offshore waveheight hazard to inundation hazard, we chose to use a numerical approach rather than existing empirical approaches because of the limitation in accuracy of the latter. We used the source disaggregation (Figure 3.2) for several regions along the California coast to select the source regions, and magnitudes that contribute the most to the hazard. Invariably, apart from the contribution of the Cascadia subduction zone on the Cascadia hazard, only three other regions are very significant: Alaska, Kamchatka-Kurile, and Chile. All subsequent scenarios were therefore done for these regions. Just using the disaggregation to select the scenarios is not sufficient, since this would not include the aleatory uncertainties in the offshore waveheight. We therefore computed a suite of scenarios with increasing amplification factors (i.e., we multiplied the slip by increasing factors) and for every region and return period chose the scenarios that yielded waveheights that bracket the probabilistic offshore waveheights. This matching is carried out using the coarse grid from the nonlinear runs (which is similar to the coarse grid from the probabilistic offshore hazard calculations) so that differences in bias between the fine and coarse grids are taken into account.

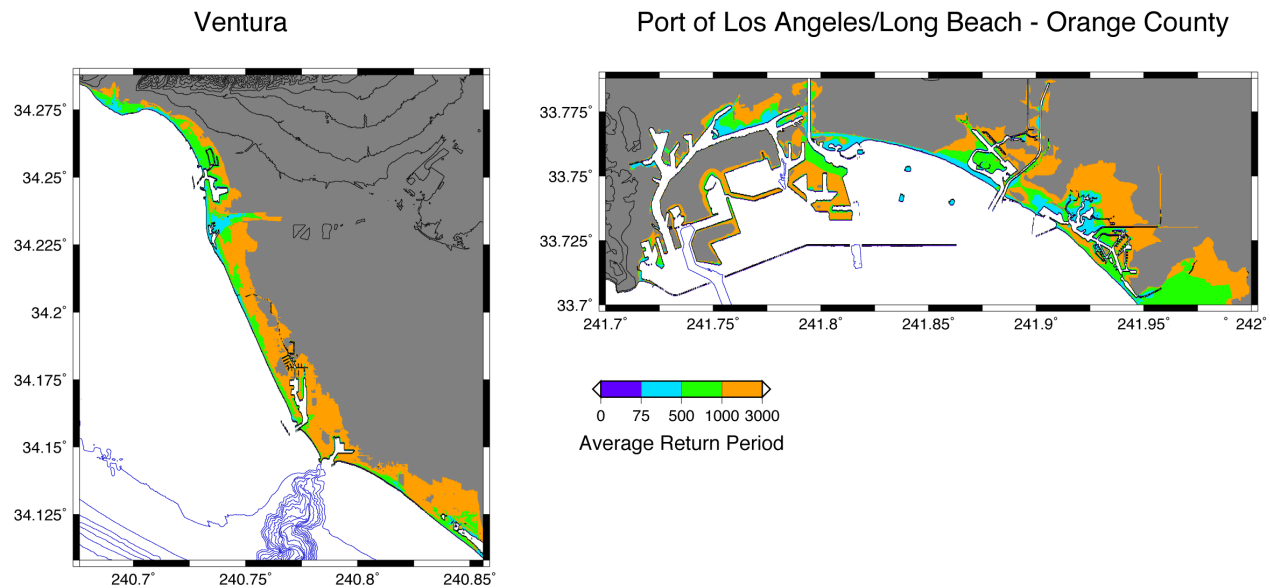


Figure 4.3. Probabilistic inundation map for two sites in Southern California, Ventura (left) and southern Los Angeles (right).

The inundation from that particular source region can then be determined by taking the weighted average of the two scenario runs that bracket the offshore waveheight. This way, we only need to compute a limited number of fully nonlinear scenarios but still retain the directional (i.e., source region specific) character and probabilistic nature of the hazard. The line of inundation can then be determined by specifying that it borders an area that is inundated by tsunami waves from all the different major source zones for that particular return period. In addition, we can also compute the local inundation level (height of the water column) exceedance for different return periods.

In Figure 4.1 – 4.3 we show several examples of these inundation maps for areas in California. Up in Cascadia, the inundation hazard is of course very high, with extensive inundation even for relatively short return periods.

REFERENCES

- Baba, T., K. Hirata, and Y. Kaneda (2004), Tsunami magnitudes determined from ocean-bottom pressure gauge data around Japan, *Geophys. Res. Lett.*, 31, L08303, doi:10.1029/2003GL019397.
- Baba, T, Cummins, P.R., Thio, H.K., and Tsushima, H., 2008. Validation and joint inversion of teleseismic waveforms for earthquake source models using deep ocean bottom pressure records: A case study of the 2006 Kuril megathrust earthquake, *Earth Plan. Sc. Lett.*, in press.
- Burbidge, D., Cummins, P.R., Mleczko, R. and Thio, H.K., 2008. A Probabilistic Tsunami Hazard Assessment for Western Australia, *Pure and Applied Geophysics*, in press.
- Fujii, Y., and K. Satake (2006), Source of the July 2006 West Java tsunami estimated from tide gauge records, *Geophys. Res. Lett.*, 33, L24317, doi:10.1029/2006GL028049.
- Hayes, D.E. and Lewis, S.D., 1984, A geophysical study of the Manila trench, Luzon, Philippines, *Journal of Geophysical Research*, v. 89, p. 9171-9195.
- Ichinose, G., P. Somerville, H. K. Thio, R. Graves, and D. O'Connell (2007), Rupture process of the 1964 Prince William Sound, Alaska, earthquake from the combined inversion of seismic, tsunami, and geodetic data, *J. Geophys. Res.*, 112, B07306, doi:10.1029/2006JB004728.
- McGuire, R., 2004. *Seismic hazard and risk analysis*, EERI Monograph, 240 pp.
- Okal, E.A. and Synolakis, C.E. (2003), A theoretical comparison of tsunamis from dislocations and landslides, *Pure and Applied Geophysics*, vol. 160, pp. 2177-2188.

- Papazachos, B.C., Scordilis, E.M., Pangiatiopoulos, D.G., Pazazachos, C.B. and Karakaisis, G.F., 2004. Global relations between seismic fault parameters and moment magnitude of earthquakes, *Bull. Geol. Soc. Greece*, XXXVI, 482,1489.
- Satake, K., 1995. Linear and Nonlinear Computations of the 1992 Nicaragua earthquake tsunami, *PAGEOH*, 144, 455-470.
- Somerville, P.G., Sato., T. and Ishii, T., 1998. Characterizing subduction zone earthquake slip models for the prediction of strong ground motion, Report to Ohsaki Research Institute, Shimizu Corp, Tokyo, Japan.
- Thio, H.K., Somerville, P., and Polet, J. (2010). Probabilistic Tsunami Hazard in California. Pacific Earthquake Engineering Research Center, PEER Report 2010/108, University of California, Berkeley.
- Thio, H.K., P. Somerville and G. Ichinose, 2007, Probabilistic Analysis of Strong Ground Motion and Tsunami Hazards in Southeast Asia. *Journal of Earthquake and Tsunami*, v. 1, No. 2, p. 119-137.
- Titov, V.V., and C.E. Synolakis, 1996. Numerical modeling of 3-D long wave run-up using VTCS-3. In *Long Wave Run-up Models*, P. Liu, H. Yeh, and C. Synolakis (eds.), World Scientific Publishing Co. Pte. Ltd., Singapore, 242–248.
- Wang, R, F. Lorenzo-Martín and F. Roth, 2003. Computation of deformation induced by earthquakes in a multi-layered elastic crust—FORTRAN programs EDGRN/EDCMP, *Computers & Geosciences*, 29, 195–207.
- Wang, R, F. Lorenzo-Martín and F. Roth, 2006. Erratum to: “Computation of deformation induced by earthquakes in a multi-layered elastic crust—FORTRAN programs EDGRN/EDCMP”, *Computers & Geosciences*, 32, 1817.
- Wells, D.L. and Coppersmith, K.J., 1994. New empirical relationships among Magnitude, Rupture Length, rupture width, rupture area and surface displacement, *Bull. Seismol. Soc. Am.*, 84, 974-1002.